CARBON 50 (2012) 2804–2809

Available at www.sciencedirect.com

SciVerse ScienceDirect

journal homepage: www.elsevier.com/locate/carbon

Exceptional negative thermal expansion and viscoelastic properties of graphene oxide paper

Yanjie Su [a], Hao Wei [a], Rungang Gao [a], Zhi Yang [a], Jing Zhang [a], Zhaohui Zhong [b], Yafei Zhang [a,*]

[a] Key Laboratory for Thin Film and Microfabrication of the Ministry of Education, Research Institute of Micro/Nano Science and Technology, Shanghai Jiao Tong University, 800 Dongchuan Road, Shanghai 200240, China

[b] Department of Electrical Engineering and Computer Science, University of Michigan, Ann Arbor, MI 48109, USA

ARTICLE INFO

Article history:
Received 13 December 2011
Accepted 16 February 2012
Available online 22 February 2012

ABSTRACT

We report unusual negative thermal expansion and viscoelastic properties in graphene oxide paper. The paper was prepared from aqueous GO dispersions using a simple vacuum evaporation technique. From room temperature to 150 °C, this paper-like graphene oxide sheet exhibits a constant negative thermal expansion coefficient of -67×10^{-6}/°C along the in-plane direction. Peculiar hysteresis loops of thermal expansion-temperature curves are observed, which are affected by the cooling rate and starting temperature of cooling. The tensile tests on GO paper show clear hysteresis loops, revealing the viscoelastic property of the paper. The viscoelastic properties show excellent frequency-stability in the range of 1.0–60 Hz. In the low temperature range −150 to 25 °C, however, they show a strong temperature dependence. The storage modulus of the graphene oxide paper continuously increases with decreasing temperature.

1. Introduction

As a single-atom-thick sheet of sp^2-hybridized carbon atoms, graphene is considered as one of the most promising candidate materials for future applications in energy storage [1], nano-electronics [2,3], and composites [4]. Graphene oxide (GO), likely the most important graphene derivative, has also been prepared by oxidizing graphite through a modified Hummers method [5]. Recent works have demonstrated that GO can be used to construct building blocks for novel applications in paper-like materials [6,7], composites [8,9], and memory devices [10,11]. To this end, GO paper has been obtained by various approaches including the flow-directed filtration [6,7,12,13], evaporation-assembly [14], spin-coating [15], and Langmuir–Blodgett assembly [16]. The experimental and theoretical studies on the mechanical properties of GO paper reveal excellent Young's modulus of 22–42 GPa [6,7,13,17] and an ultimate tensile strength of 43–130 MPa [6,7,13,17], which are significantly higher than those of bucky paper [18]. Despite these pioneer works, the frequency and temperature responses of the mechanical properties of GO paper are also important factors needed to be considered for potential thermal and mechanical applications. However, the thermal expansion behavior of GO paper in a wide temperature range has not been studied in detail. There are also no reports on the temperature dependent strain–stress relation on GO paper to the best of our knowledge.

In this paper, we demonstrate the fabrication of free-standing GO paper by simple vacuum evaporation of water from aqueous GO dispersions. The thermal expansion behavior was examined in detail by measuring the variation of GO paper dimensions under temperature cycle. We further

* *Corresponding author:* Fax: +86 21 3420 5665.
E-mail address: yfzhang@sjtu.edu.cn (Y. Zhang).
0008-6223/$ - see front matter
doi:10.1016/j.carbon.2012.02.045

conducted the experimental study on the viscoelastic properties through monitoring storage modulus, loss modulus and damping ratio at different frequency and temperature.

2. Experimental

2.1. Preparation of GO and GO paper

Graphene oxide was synthesized by oxidation of highly oriented pyrolytic graphite (HOPG) powder through a modified Hummers method [5]. The as-obtained GO sheets were dispersed into deionized water (100 ml of a 10 mg/ml solution) with the aid of ultrasonication (200 W for 60 min). The homogeneous dispersion of GO sheets was poured into a watch-glass with 15 cm in diameter, and then the watch-glass was transferred into vacuum oven, followed by slowly evacuating to 5 Pa and maintaining the vacuum for about 24–48 h at 45 °C. Finally, the as-prepared GO paper was peeled from the watch-glass, and GO paper was cut into strips.

2.2. Characterization

Transmission electron microscopy (TEM) observations were carried out in a JEOL JEM-2100 instrument operating at 200 kV. Dynamic mechanical tests were conducted with a dynamic mechanical analyzer (Q800 DMA, TA Instruments). After drying at 80 °C for 24 h, the samples were griped using film tension clamps with a clamp compliance of ca.0.260 μm/N. The thermal expansion was characterized under air atmosphere with a preload of 0.01 N and a temperature ramp rate of ±5 °C/min. The response of viscoelasticity to frequency was measured by changing frequency from 1.0 to 60 Hz with a constant strain of 0.1% at different temperature. The response of viscoelasticity to temperature was tested by changing temperature from 25 to 150 °C with a constant strain of 0.1% and frequency of 1.0 Hz. All tensile tests were performed in controlled-force mode with a preload of 0.01 N, and force was loaded with a force ramp rate of 2.0 N/min. The sample diameter was measured using standard calipers. The length between the clamps was measured by the DMA instrument.

3. Results and discussion

GO papers were prepared through vacuum drying of colloidal dispersions of GO sheets in a watch-glass. The diameter and thickness of GO papers can be rationally designed by controlling the diameter of watch-glass and the amount of colloidal dispersions. The morphology of as-obtained 15 cm diameter GO paper is shown in Fig. 1a; and a 25-μm-thick GO paper strip of 0.75 cm by 14 cm is shown in Fig. 1b. TEM images (Fig. 1c) show that the average dimensions of individual GO sheet is about 5 × 5 μm. The wrinkled surface can be clearly observed, which can play an important role in enhancing mechanical interlocking and load transfer within the matrix [6].

The thermal expansion properties of graphene and GO are important parameters for their applications in nano-mechanical devices, which are affected by atomic vibration frequency, internal stress, entropy, etc. [18,19]. We first investigated the

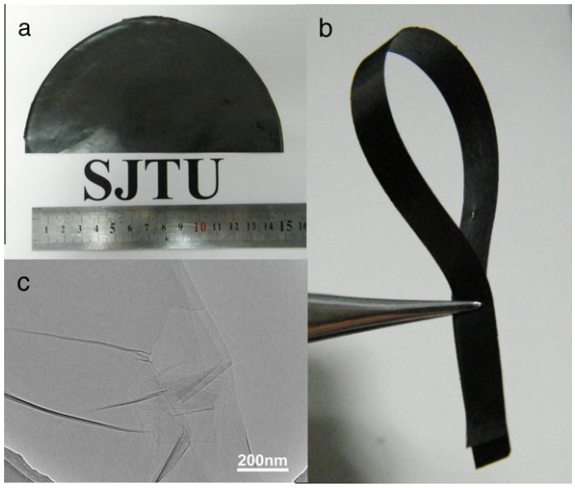

Fig. 1 – (a and b) Morphology of GO paper; (c) TEM image of GO sheets.

linear parameter of thermal expansion (PTE) β_T of GO papers from 30 to 300 °C (Fig. 2a). β_T is defined as:

$$\beta_T = \frac{L_{(T)} - L_{(T_0)}}{L_{(T_0)}} \quad (1)$$

where $L_{(T)}$ and $L_{(T_0)}$ are the lengths of sample at temperatures T and T_0.The coefficient of thermal expansion (CTE) α_T can then be estimated as:

$$\alpha_T \approx \frac{\Delta\beta_T}{\Delta T} \quad (2)$$

Our experimental results show the variations of the CTE values depend on the temperature range. From 30 to 160 °C, the CTE value remains a constant negative number (about -67×10^{-6}/°C) along the in-plane direction, which is similar to the previously reported values measured by Dikin et al. [6]. As we know, monolayer graphene sheet possesses negative thermal expansion coefficient due to negative in-plane lattice parameter [20,21]. As graphene derivative, GO sheets also possess similar thermal expansion properties [6]. The negative thermal expansion of GO paper thus can be explained from the collective effect of numerous GO sheets with negative thermal expansion. Interestingly, when the temperature is raised beyond 160 °C, the CTE value quickly drops and reach $\sim -1208 \times 10^{-6}$/°C at ~230 °C. The more negative CTE value at higher temperature is likely caused by the thermal expansion of interlayer gas (Fig. 3), which results in large thermal contraction along GO paper. The structural deformation due to thermal reduction of GO [2,22,23] may also contribute to the negative CTE, and further study is needed to understand detailed mechanism. We also note that increases in temperature beyond 230 °C result in drastic oxidization of GO under air atmosphere.

The response of thermal expansion to temperatures was also investigated by temperature cycles from −150 °C to room temperature (Fig. 2b and c). Contrary to the heating process from room temperature to 300 °C, thermal expansion-temperature cycles show two distinct paths corresponding to the cooling and heating process, respectively, which is called "hysteresis loop" of thermal expansion. The inflections of

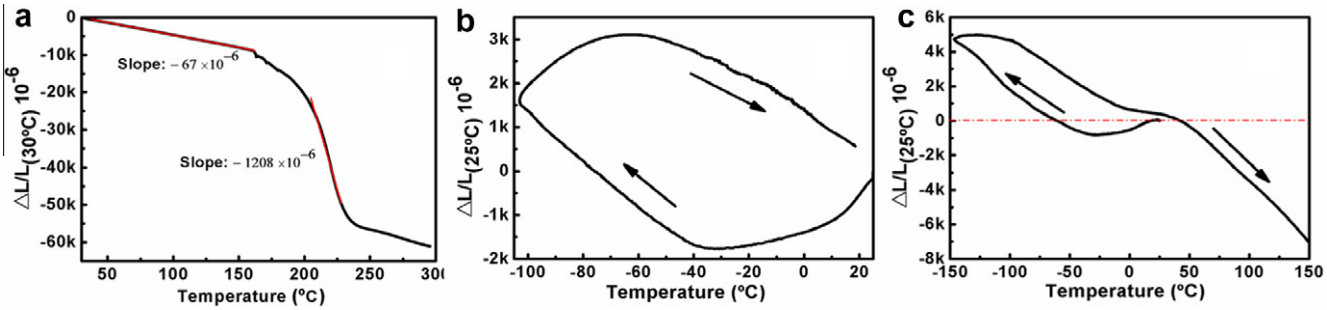

Fig. 2 – Thermal expansion curves of GO paper with a ramping rate of 5 °C/min. (a) The sample was heated to 300 °C; (b) temperature cycle varies from room temperature to −100 °C; (c) temperature cycle varies in the range from −150 to 150 °C.

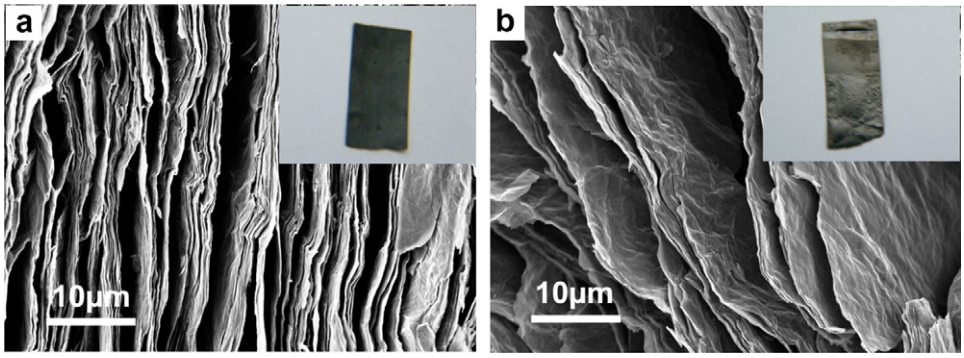

Fig. 3 – SEM images and Digital photo (Insets) of GO papers. (a) Pristine sample; (b) after DMA measurement at 150 °C.

CTE value from positive to negative can be clearly observed during both the cooling and heating processes. To verify the repeatability of peculiar thermal expansion, we further investigated the response curves of thermal expansion to the starting temperature for cooling and to the cooling rate in Fig. 4. One can see clearly that the inflection temperature of CTE curve is affected by the cooling rate and starting temperature of cooling. When cooling process starts from a low enough temperature or with a faster ramp rate, the inflections of CTE value disappear. To eliminate the influence of free water, the GO paper was dried again under vacuum at 100 °C for 60 h and the measurements were repeated. The results suggest that the inflection temperature of CTE curve is still affected by the cooling rate and starting temperature of cooling (Fig. 4b), indicating that free water inside the GO paper samples does not play a role in the thermal expansion behavior. Based on these experimental results, we think the hysteresis loop may result from the competing effects of in-plane expansion and contraction perpendicular to uniaxial tension during thermal cycling. Interlayer trapped gas molecules can also cause hysteretic temperature loop. In addition, the hysteretic thermal expansion behavior can also result from hydrogen bond networks, water molecules inside GO sheets and other factors related to the microstructure and density of GO paper [20,21,24–27]. Further detailed investigation needs to be done in subsequent studies.

We further performed tensile tests on GO paper using film tension clamps in controlled-force mode. At room temperature, the ultimate tensile strength of GO paper is about 80 MPa, which is similar to the previously reported value [7]. Fig. 5 shows the results of strain–stress cyclic curves of GO paper at different temperatures. The tensile strain of GO paper increases as increasing temperature, and the Young's moduli are 21.5, 12.3, and 3.3 GPa, at −150, 25, and 150 °C, respectively. At lower temperature (Fig. 5a), GO paper becomes more compact due to the contraction perpendicular to uniaxial tension direction and the expansion parallel to uniaxial tension direction, which results in a lower tensile strain [28]. At higher temperature (Fig. 5c), GO paper is tightened due to the contraction of GO sheets and the expansion perpendicular to uniaxial tension direction. Interlayer slip between GO sheets happen easily, resulting in larger residual strain when unloaded. Importantly, Fig. 5 also show clear hysteresis loops of strain–stress curves, indicating the viscoelastic behavior of GO paper [6,29]. The larger integration area beneath the strain–stress curve as temperature increases corresponds to more energy dissipated in load–unload process.

We further investigate the viscoelastic properties including storage modulus, loss modulus, and damping ratio ($\tan\delta$) under different frequencies and temperatures. The frequency responses of the storage modulus, loss modulus, and damping ratio of GO paper in the temperature range from −150 to 150 °C are shown in Fig. 6a–c. The viscoelastic properties exhibit higher stiffness (storage modulus = 14 GPa), smaller dissipation (loss modulus = 1.2 GPa), and lower damping ratio ($\tan\delta$ = 0.086) than those of carbon nanotubes [1] at room temperature. Frequency dependence viscoelastic properties tests show flat responses in frequency range of 1.0–60 Hz at

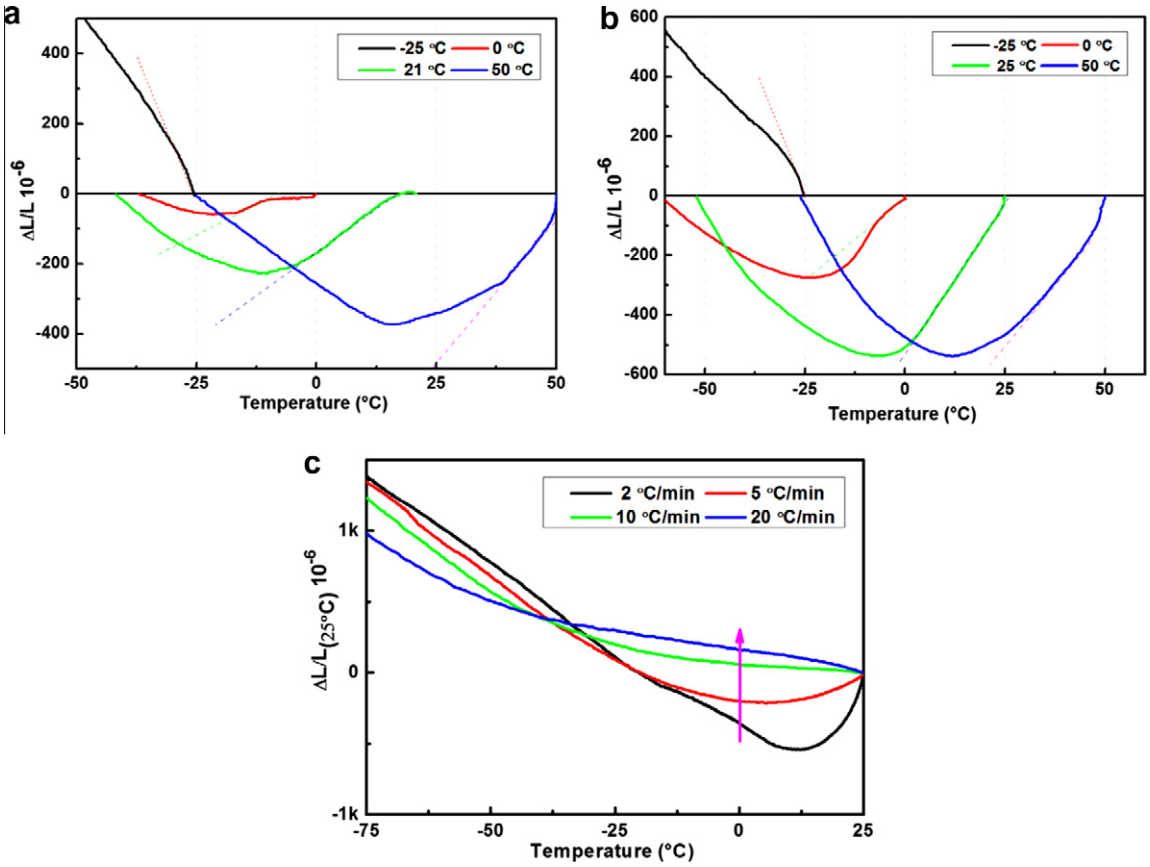

Fig. 4 – The response curves of thermal expansion to temperatures with a ramping rate of 5 °C/min during the cooling processes from different temperatures. (a) After drying at 80 °C for 24 h; (b) after secondary drying at 100 °C for 60 h. (c) The response curves of thermal expansion to temperatures with different ramping rates during the cooling processes.

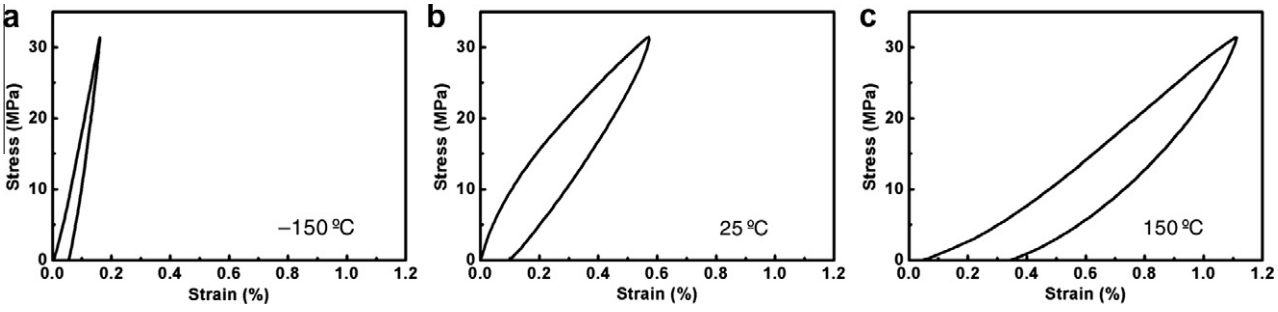

Fig. 5 – Strain–stress cyclic curves of GO paper at −150, 25, and 150 °C under controlled force varying from 0 to 5.0 N with a force ramp rate of 2.0 N/min.

temperature below 150 °C. We also study the temperature dependence of the viscoelastic properties (Fig. 6d–f). Stronger temperature dependence is observed at temperature below about 25 °C. The storage modulus increases with decreasing temperature and reaches the highest value of 35 GPa at −150 °C, while loss modulus and damping ratio decrease with lowering temperature. In the temperature range from room temperature to 150 °C, however, the viscoelastic properties are highly stable and insensitive to temperature changes. The viscoelastic stability at higher temperature region promises GO paper for room temperature applications.

4. Conclusions

In conclusion, we study the negative thermal expansion and temperature dependent viscoelastic properties of GO paper. The free-standing paper was prepared by vacuum evaporating water from aqueous GO dispersions. The coefficient of the in-plane thermal expansion is found to be $\sim -67 \times 10^{-6}$/°C from room temperature to 160 °C, and decreases sharply when temperature is raised above 160 °C. In the low temperature range −150 to 25 °C, peculiar hysteresis loops of thermal expansion-temperature curves are observed, which are affected by

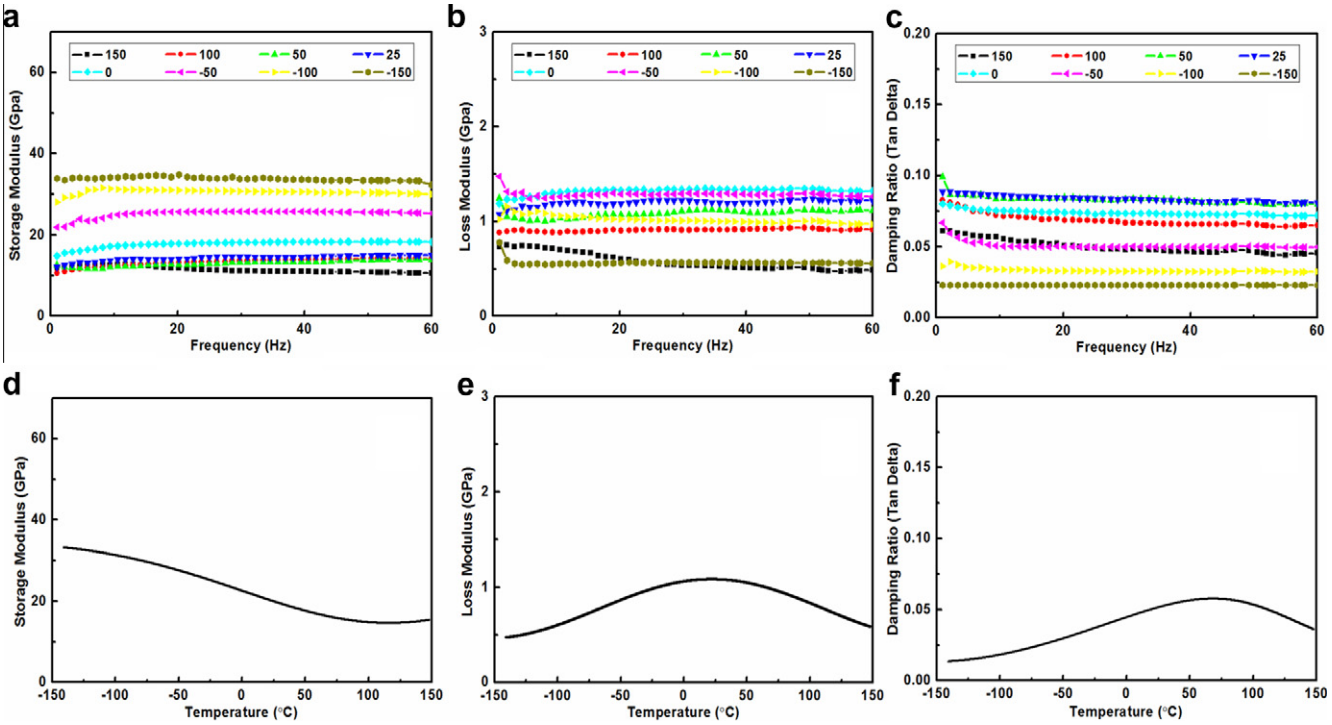

Fig. 6 – Viscoelastic properties of the GO paper at different temperatures. (a–c) Storage modulus, loss modulus, and damping ratio as function of frequency (1.0–60 Hz) at temperatures from −150 to 150 °C. (d) Storage modulus, (e) loss modulus, and (f) damping ratio as function of temperature (−150 to 150 °C) with a constant strain of 0.1% and a constant frequency of 1 Hz.

the cooling rate and starting temperature of cooling. The tensile tests show increasing Young's modulus with reducing temperature, with the highest value of 21.5 GPa is obtained at −150 °C. The viscoelastic properties exhibit preferable frequency stability from 1.0 to 60 Hz, and preferable temperature stability from room temperature to 150 °C. At temperature below about 25 °C, however, the storage modulus increases with decreasing temperature, while loss modulus and damping ratio decrease with lowering temperature. Our findings of the peculiar thermal expansion and viscoelastic properties of GO paper not only contribute to the fundamental understanding of the thermal and mechanical properties at low dimension, but also pave the way toward GO paper based thermal and mechanical applications.

Acknowledgements

We acknowledge financial supports from the National Natural Science Foundation of China (No. 50730008, 61006002 and 50902092), Shanghai Science and Technology Grant (No. 09JC1407400, 1052nm02000, and 1052nm06800), and the support from the U-M/SJTU Collaborative Research Program in Renewable Energy Science and Technology.

REFERENCES

[1] Liu CG, Yu ZN, Neff D, Zhamu A, Jang BZ. Graphene-based supercapacitor with an ultrahigh energy density. Nano Lett. 2010;10:4863–8.

[2] Wei ZQ, Wang DB, Kim S, Kim SY, Hu YK, Yakes MK, et al. Nanoscale tunable reduction of graphene oxide for graphene electronics. Science 2010;328:1373–6.

[3] Lee S, Lee K, Zhong ZH. Wafer scale homogeneous bilayer graphene films by chemical vapor deposition. Nano Lett 2010;10:4702–7.

[4] Stankovich S, Dikin DA, Dommett GHB, Kohlhaas KM, Zimney EJ, Stach EA, et al. Graphene–based composite materials. Nature 2006;442:282–6.

[5] Hummers Jr WS, Offeman RE. Preparation of graphitic oxide. J Am Chem Soc 1958;80:1339.

[6] Dikin DA, Stankovich S, Zimney EJ, Piner R, Dommett GHB, Evmenenko G, et al. Preparation and characterization of graphene oxide paper. Nature 2007;448:457–60.

[7] Park S, Lee KS, Bozoklu G, Cai WW, Nguyen ST, Ruoff RS. Graphene oxide papers modified by divalent ions–enhancing mechanical properties via chemical cross-linking. ACS Nano 2008;2:572–8.

[8] Compton OC, Nguyen ST. Graphene oxide, highly reduced graphene oxide, and graphene: versatile building blocks for carbon-based materials. Small 2010;6:711–23.

[9] Chen S, Zhu JW, Wu XD, Han QF, Wang X. Graphene oxide–MnO_2 nanocomposites for supercapacitors. ACS Nano 2010;4:2822–30.

[10] Jeong HY, Kim JY, Kim JW, Hwang JO, Kim JE, Lee JY, et al. Graphene oxide thin films for flexible nonvolatile memory applications. Nano Lett 2010;10:4381–6.

[11] Hong SK, Kim JE, Kim SO, Choi SY, Cho BJ. Flexible resistive switching memory device based on graphene oxide. IEEE Electron Device Lett 2010;31:1005–7.

[12] Stankovich S, Dikin DA, Compton OC, Dommett GHB, Ruoff RS, Nguyen ST. Systematic post-assembly modification of graphene oxide paper with primary alkylamines. Chem Mater 2010;22:4153–7.

[13] Compton OC, Dikin DA, Putz KW, Brinson LC, Nguyen ST. Electrically conductive "alkylated" graphene paper via chemical reduction of amine-functionalized graphene oxide paper. Adv Mater 2010;22:892–6.
[14] Chen CM, Yang QH, Yang YG, Lv W, Wen YF, Hou PX, et al. Self-assembled free-standing graphite oxide membrane. Adv Mater 2009;21:3007–11.
[15] Luo ZT, Lu Y, Somers LA, Johnson ATC. High yield preparation of macroscopic graphene oxide membranes. J Am Chem Soc 2009;131:898–9.
[16] Kulkarni DD, Choi I, Singamaneni SS, Tsukruk VV. Graphene oxide- polyelectrolyte nanomembranes. ACS Nano 2010;4:4667–76.
[17] Chen HQ, Müller MB, Gilmore KJ, Wallace GG, Li D. Mechanically strong, electrically conductive, and biocompatible graphene paper. Adv Mater 2008;20:3557–61.
[18] Berhan L, Yi YB, Sastry AM, Munoz E, Selvidge M, Baughman R. Mechanical properties of nanotube sheets: alterations in joint morphology and achievable moduli in manufacturable materials. J Appl Phys 2004;95:4335–45.
[19] Suleimanov RA, Abdullaev NA. The nature of negative linear expansion of graphite crystals. Carbon 1993;31:1011–3.
[20] Mounet N, Marzari N. First-principles determination of the structural, vibrational and thermodynamic properties of diamond, graphite, and derivatives. Phys Rev B 2005;71:205–14.
[21] Zakharchenko KV, Los JH, Katsnelson MI, Fasolino A. Atomistic simulations of structural and thermodynamic properties of bilayer graphene. Phys Rev B 2010;81:235439–46.
[22] Zhu YW, Stoller MD, Cai WW, Velamakanni A, Piner RD, Chen D, et al. Exfoliation of graphite oxide in propylene carbonate and thermal reduction of the resulting graphene oxide platelets. ACS Nano 2010;4:1227–33.
[23] Jung I, Dikin DA, Piner RD, Ruoff RS. Tunable electrical conductivity of individual graphene oxide sheets reduced at "low" temperatures. Nano Lett 2008;8:4283–7.
[24] Medhekar NV, Ramasubramaniam A, Ruoff RS, Shenoy VB. Hydrogen bond networks in graphene oxide composite paper: structure and mechanical properties. ACS Nano 2010;4(4):2300–6.
[25] Acik M, Mattevi C, Gong C, Lee G, Cho K, Chhowalla M, et al. The role of intercalated water in multilayered graphene oxide. ACS Nano 2010;4(10):5861–8.
[26] Singh V, Sengupta S, Solanki HS, Dhall R, Allain A, Dhara S, et al. Probing thermal expansion of graphene and modal dispersion at low-temperature using graphene NEMS resonators. Nanotechnology 2010;21:165204–8.
[27] Zakharchenko KV, Katsnelson MI, Fasolino A. Finite temperature lattice properties of graphene beyond the quasiharmonic approximation. Phys Rev Lett 2009;102:046808–14.
[28] Zhao H, Min K, Aluru NR. Size and chirality dependent elastic properties of graphene nanoribbons under uniaxial tension. Nano Lett 2009;9:3012–5.
[29] Leng Y, Gu JL, Cao WQ, Zhang TY. Influences of density and flake size on the mechanical properties of flexible graphite. Carbon 1998;36:875–81.